Structure, Vol. 13, 1643–1651, November, 2005, ©2005 Elsevier Ltd All rights reserved. DOI 10.1016/j.str.2005.07.019

Crystal Structure of a Complex between Protein Tyrosine Phosphatase 1B and the Insulin Receptor Tyrosine Kinase

Shiqing Li,[1,4] Rafael S. Depetris,[1] David Barford,[2] Jonathan Chernoff,[3] and Stevan R. Hubbard[1,*]

[1]Structural Biology Program
Skirball Institute of Biomolecular Medicine and
Department of Pharmacology
New York University School of Medicine
New York, New York 10016

[2]Section of Structural Biology
Institute of Cancer Research
Chester Beatty Laboratories
London SW3 6JB
United Kingdom

[3]Fox Chase Cancer Center
Philadelphia, Pennsylvania 19111

Summary

Protein tyrosine phosphatase 1B (PTP1B) is a highly specific negative regulator of insulin receptor signaling in vivo. The determinants of PTP1B specificity for the insulin receptor versus other receptor tyrosine kinases are largely unknown. Here, we report a crystal structure at 2.3 Å resolution of the catalytic domain of PTP1B (trapping mutant) in complex with the phosphorylated tyrosine kinase domain of the insulin receptor (IRK). The crystallographic asymmetric unit contains two PTP1B-IRK complexes that interact through an IRK dimer interface. Rather than binding to a phosphotyrosine in the IRK activation loop, PTP1B binds instead to the opposite side of the kinase domain, with the phosphorylated activation loops sequestered within the IRK dimer. The crystal structure provides evidence for a noncatalytic mode of interaction between PTP1B and IRK, which could be important for the selective recruitment of PTP1B to the insulin receptor.

Introduction

Insulin activates intracellular signaling pathways that regulate cellular metabolism and growth (Saltiel and Pessin, 2002). The actions of insulin are mediated by its transmembrane receptor, an $\alpha_2\beta_2$ glycoprotein and member of the receptor tyrosine kinase (RTK) family of cell surface receptors (Ebina et al., 1985; Ullrich et al., 1985). Insulin binding to the extracellular α chains induces a structural change within the receptor, facilitating autophosphorylation of specific tyrosine residues in the cytoplasmic portion of the β chains. Tyrosine phosphorylation increases the catalytic activity of the receptor and also generates recruitment sites for downstream signaling proteins, such as the insulin receptor substrate (IRS) proteins (White, 1998), Shc (Gustafson et al., 1995), APS (Ahmed et al., 1999; Moodie et al., 1999), and SH2-B (Kotani et al., 1998).

*Correspondence: hubbard@saturn.med.nyu.edu

[4]Present address: Department of Physiology, University of Pennsylvania School of Medicine, Philadelphia, Pennsylvania 19104.

A large family of protein tyrosine phosphatases (PTPs), including both receptor and nonreceptor types, serves to attenuate activated RTK signaling pathways, or to maintain basal-level phosphorylation levels, by dephosphorylating RTKs as well as their substrate proteins (Tonks and Neel, 1996). In cell culture experiments, several PTPs, including LAR, PTPα, and PTP1B have been shown to be capable of dephosphorylating the insulin receptor (Asante-Appiah and Kennedy, 2003). An important advance in our understanding of insulin receptor downregulation in vivo came from the generation of PTP1B-deficient mice (Elchebly et al., 1999; Klaman et al., 2000). Despite the ability of PTP1B to dephosphorylate numerous growth factor receptors in vitro and in cells, the PTP1B-deficient mice are of normal size (i.e., no overgrowth phenotype) and exhibit only two apparent phenotypes: a hypersensitivity to insulin, due to prolonged insulin receptor phosphorylation, and resistance to weight gain on a high-fat diet, through sustained activity of Jak2 associated with the leptin receptor (Myers et al., 2001; Zabolotny et al., 2002). The mice knockout studies established that PTP1B has highly specific targets in vivo, one of which is the insulin receptor.

PTP1B is a cytoplasmic, nonreceptor PTP that is tethered to the endoplasmic reticulum (ER) by a hydrophobic sequence at its C terminus (Tonks, 2003). While many nonreceptor PTPs are targeted to their substrates via recognizable protein interaction modules, such as the Src homology-2 (SH2) domains in SHP2, PTP1B has few obvious recruitment domains/motifs, except for a proline-rich region C-terminal to the catalytic domain, which binds SH3 domain-containing proteins such as $p130^{Cas}$ (Liu et al., 1996). PTP1B is ubiquitously expressed in vertebrates, and many RTKs undergo ligand-stimulated endocytosis, which would bring receptors in proximity to the ER. Therefore, PTP1B specificity for the insulin receptor does not derive from tissue-specific coexpression or from a unique subcellular colocalization. Rather, specificity likely arises from intrinsic substrate (catalytic) preferences, i.e., the sequence context of phosphorylation sites in the insulin receptor, and/or targeting of PTP1B to the insulin receptor through noncatalytic protein-protein interactions.

Previous crystallographic and biochemical studies of the interaction between a PTP1B trapping mutant (which binds to but does not hydrolyze phosphotyrosine) and a phosphopeptide representing the activation loop of the insulin receptor kinase domain (IRK) indicated that the tandem phosphotyrosine residues pY1162 and pY1163 in the kinase activation loop are important determinants of specificity, and that the N- and C-terminal flanking residues, aspartic acid and arginine, might also contribute (Salmeen et al., 2000). Because numerous RTKs, particularly the highly related insulin-like growth factor-1 (IGF1) receptor, fibroblast growth factor receptor-1-4, TrkA/B/C, and MuSK, possess tandem activation loop tyrosines in a similar sequence context, (D/E)YY(R/K), it is unlikely that this sequence motif is sufficient to account for the observed in vivo specificity of PTP1B for the insulin receptor.

Biochemical studies originally aimed at probing insulin-stimulated PTP1B tyrosine phosphorylation had shown that mutation of two tyrosine residues in the catalytic domain of PTP1B, Y152 and Y153, reduced the interaction between a PTP1B trapping mutant and the insulin receptor (Bandyopadhyay et al., 1997). Subsequent studies demonstrated that the PTP1B Y152F/Y153F double mutant was much less efficient at dephosphorylating the insulin receptor than wild-type PTP1B, yet these phenylalanine substitutions had no effect on PTP1B dephosphorylation of a control phosphopeptide or of $p130^{Cas}$ (Dadke et al., 2000; Dadke and Chernoff, 2002). These studies provided evidence for interactions between PTP1B and the insulin receptor that are distal to the PTP1B active site.

In an effort to elucidate further the molecular determinants of PTP1B specificity for the insulin receptor, we have cocrystallized a trapping mutant of PTP1B with phosphorylated IRK. The crystal structure of the complex shows an unanticipated mode of interaction between PTP1B and IRK, in which PTP1B binds not to a phosphotyrosine in the IRK activation loop, but rather to the opposite side of the kinase domain. The PTP1B-IRK interface comprises residues that are highly characteristic for these two proteins, including Y152 and Y153 of PTP1B. The PTP1B-IRK crystal structure indicates that a noncatalytic mode of interaction between PTP1B and the insulin receptor could play an important role in the in vivo specificity of PTP1B for the insulin receptor.

Table 1. X-Ray Data Collection and Refinement Statistics

Data Collection	
Resolution (Å)	30.0–2.3
Observations	208,286
Unique reflections	60,480
Completeness[a] (%)	98.1 (94.2)
R_{sym}[a,b] (%)	10.4 (27.2)
$\langle I/\sigma I \rangle$	8.0
Refinement[c]	
Resolution (Å)	30.0–2.3
Reflections	58,237
R_{cryst}/R_{free}[d] (%)	20.8/23.9
Rms deviations	
Bond lengths (Å)	0.006
Bond angles (°)	1.3
B factors[e] ($Å^2$)	1.1
Average B factors ($Å^2$)	
All atoms	23.4
PTP1B	21.8
IRK	24.8
Water	24.5
Sulfate	36.2

[a] The overall (30–2.3 Å) value is given first, with the value in the highest resolution shell (2.38–2.30 Å) given in parenthesis.
[b] $R_{sym} = 100 \times \Sigma|I - \langle I \rangle|/\Sigma I$.
[c] Atomic model includes 1161 residues (9216 atoms), 10 sulfate ions (50 atoms), and 377 water molecules (377 atoms).
[d] $R_{cryst} = 100 \times \Sigma||F_o| - |F_c||/\Sigma|F_o|$, where F_o and F_c are the observed and calculated structure factors, respectively ($F_o > 0\sigma$). R_{free} was determined from 5% of the data.
[e] For bonded protein atoms.

Results

Overall Structure of the PTP1B-IRK Complex

For cocrystallization trials, we used a C215A trapping mutant of PTP1B (residues 1–298) and tris-phosphorylated IRK (residues 978–1283) in which Y1158, Y1162, and Y1163 in the activation loop were phosphorylated. Orthorhombic crystals were obtained at pH 7.5 in ammonium sulfate. The crystal structure of the complex was solved by molecular replacement by using the individual structures of PTP1B (Salmeen et al., 2000) and tris-phosphorylated IRK (Hubbard, 1997) as search models. The structure has been refined at 2.3 Å resolution with an R_{cryst} value of 21% (R_{free} value of 24%). Data collection and refinement statistics are given in Table 1. The crystallographic asymmetric unit comprises two molecules each of PTP1B and IRK, arranged as a symmetric dimer of two 1:1 PTP1B-IRK complexes that interact through an IRK dimer interface (Figure 1).

In the previous crystal structure of PTP1B in complex with a phosphopeptide representing the IRK activation loop (Salmeen et al., 2000), pY1162 is bound in the active site of the PTP1B trapping mutant, poised for dephosphorylation. This structure is indicative of a catalytic mode of interaction between PTP1B and its substrate phosphopeptide. The striking feature of the present PTP1B-IRK structure is the binding of PTP1B to the "backside" of the kinase domain rather than to a phosphotyrosine in the activation loop ("front" side). This mode of binding between PTP1B and IRK is evidently facilitated by crystallization in ammonium sulfate, which effectively competes with the activation loop phosphotyrosines for PTP1B binding; a well-ordered sulfate ion is bound in the PTP1B active site. Thus, the present structure represents a noncatalytic mode of interaction between PTP1B and IRK.

PTP1B-IRK Interface

The interface between PTP1B and IRK, which is nearly identical in the two copies of PTP1B-IRK present in the asymmetric unit, buries a total surface area of ~1725 $Å^2$, with a shape complementarity value of 0.70 (Lawrence and Colman, 1993). These values are on par with biologically relevant protein-protein interactions, such as antibody-antigen complexes (Janin and Chothia, 1990). There are two main PTP1B-IRK interaction regions that encompass both the N- and C-terminal lobes of IRK: the β2-β3 loop of IRK (N-terminal lobe) with the β9-β10 turn of PTP1B, and α helix J (αJ) of IRK (C-terminal lobe) with the WPD loop (between β11 and α2) of PTP1B (Figure 1).

The key interaction between the N-terminal lobe of IRK and PTP1B is the hydrogen bond between E1022 (denoted $E1022^I$) in the β2-β3 loop of IRK and Y152 (denoted $Y152^P$) in the β9-β10 turn of PTP1B (Figure 2B). $N193^P$ (α3) also contacts the β2-β3 loop of IRK, making a hydrogen bond with the backbone of $G1021^I$ and a water-mediated hydrogen bond with the backbone of $A1023^I$. $Y153^P$ (β10) is in van der Waals contact with the backbone of $G1021^I$. Two intramolecular interactions favorably position $Y152^P$ and $E1022^I$ for hydrogen bonding with each other: $N193^P$ is hydrogen bonded to $Y152^P$, and $T1025^I$ (β3) is hydrogen bonded to $E1022^I$ (Figure 2B).

The WPD loop of PTP1B (residues 179–184), which contains the PTP-conserved catalytic residue D181,

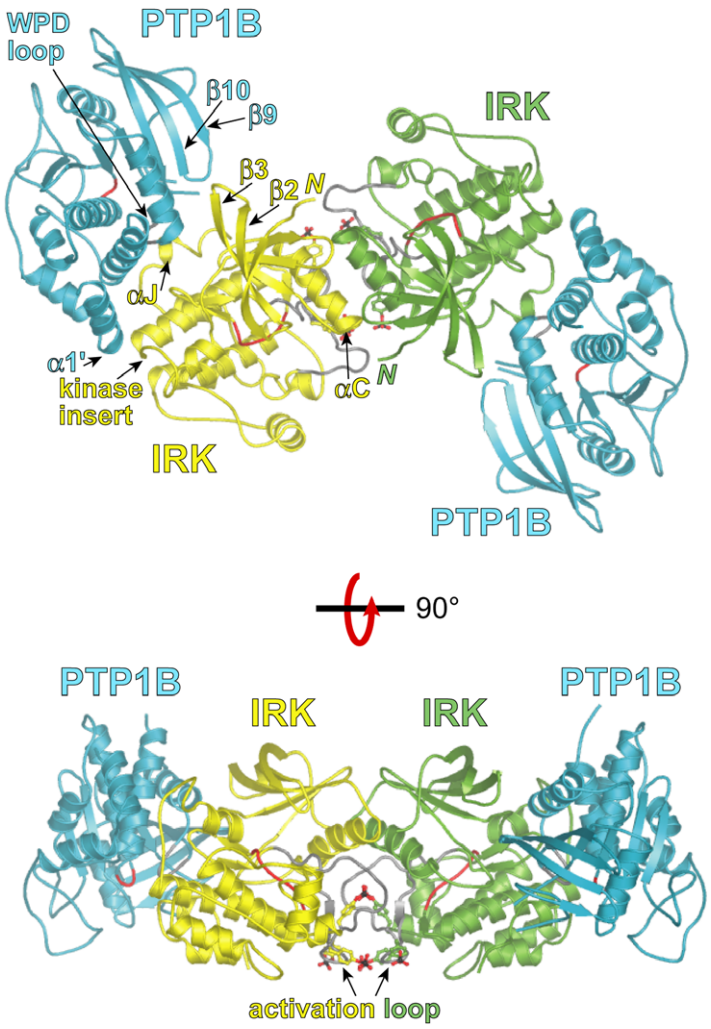

Figure 1. Ribbon Diagram of the PTP1B-IRK Crystal Structure

The two PTP1B molecules are colored cyan, and the two IRK molecules are colored yellow and green. The catalytic loops of PTP1B (residues 215–218) and IRK (residues 1130–1137) are colored red, and the WPD loop of PTP1B (residues 179–184) and the activation loop of IRK (residues 1150–1171) are colored gray. The activation loop phosphotyrosines of IRK are shown in ball-and-stick representation, with carbon atoms colored yellow or green, oxygen atoms colored red, and phosphorus atoms colored black. Select secondary structure elements are indicated in one of the two 1:1 PTP1B-IRK complexes in the top panel. The N termini of the IRK molecules, which would lead into the juxtamembrane region and transmembrane helix of the insulin receptor, are labeled "*N*." In the top panel, the noncrystallographic 2-fold axis is perpendicular to the page, and in the bottom panel, the 2-fold axis is vertical, in the plane of the page. Figures 1–4 were rendered with Pymol software (www.pymol.org).

makes several contacts with residues in and preceding αJ of IRK (Figure 2C), a helix that is unique to the insulin receptor subfamily of RTKs. Hydrophobic packing interactions in this interface include $P180^{P}$ (WPD loop) with $V1274^{I}$ (αJ) and $F182^{P}$ (WPD loop) with $P1269^{I}$. Additional interactions in this region include a salt bridge between $K120^{P}$ (β6-β7 loop) and $E1273^{I}$ (αJ), a hydrogen bond between $R112^{P}$ (β4-β5 loop) and the backbone of $E1273^{I}$, and a hydrogen bond between $H1268^{I}$ (αI-αJ loop) and the backbone of $F182^{P}$. These interactions between αJ of IRK and the WPD loop promote a closed conformation of this catalytically important loop, which typically adopts an open conformation in the absence of a phosphotyrosine in the catalytic site.

Additional interactions in the PTP1B-IRK interface include the β7-β8 loop of IRK (C-terminal lobe) with the β11-α2 loop of PTP1B (Figure 2C) and the kinase insert region of IRK (αD-αE loop) with α1′ of PTP1B (Figure 1). A full listing of the interactions in the PTP1B-IRK interface is given in Table 2.

Comparison of the PTP1B Structure with Previous Structures

A superposition of the PTP1B structure from the PTP1B-IRK complex with the PTP1B structure with the bound IRK activation loop phosphopeptide (Salmeen et al., 2000) (PDB code 1G1F) reveals a very similar overall conformation, with a root mean square deviation of 0.6 Å for 270 Cα atoms, but with several notable differences (Figure 3). The most conspicuous difference is the behavior of the C-terminal segment of PTP1B, residues 283–298. In previous crystal structures of PTP1B with a phosphotyrosine ligand bound in the active site (e.g., PDB code 1G1F), the WPD loop adopts a closed conformation, and residues in the C-terminal segment form an α helix (α7), which interacts with α3 and the β9-β10 turn. Conversely, in structures of apo PTP1B or PTP1B with an ion bound in the active site (e.g., PDB code 2HNQ [Barford et al., 1994]), the WPD loop adopts an open conformation, and the C-terminal segment is disordered. In the PTP1B-IRK structure, despite the WPD loop adopting a closed conformation, residues 283–298 are disordered. The interaction between the β2-β3 loop of IRK and the β9-β10 turn of PTP1B evidently displaces α7 of PTP1B (Figure 3), causing its disordering. Interestingly, a recently described allosteric inhibitor of PTP1B also displaces α7, which impairs closure of the WPD loop (Wiesmann et al., 2004).

Another difference in the PTP1B structure as compared to previous structures is the β5/β6 region (residues 111–120) (Figure 3B). Residues 115–117 are disordered in the PTP1B-IRK complex, and residues 112–114

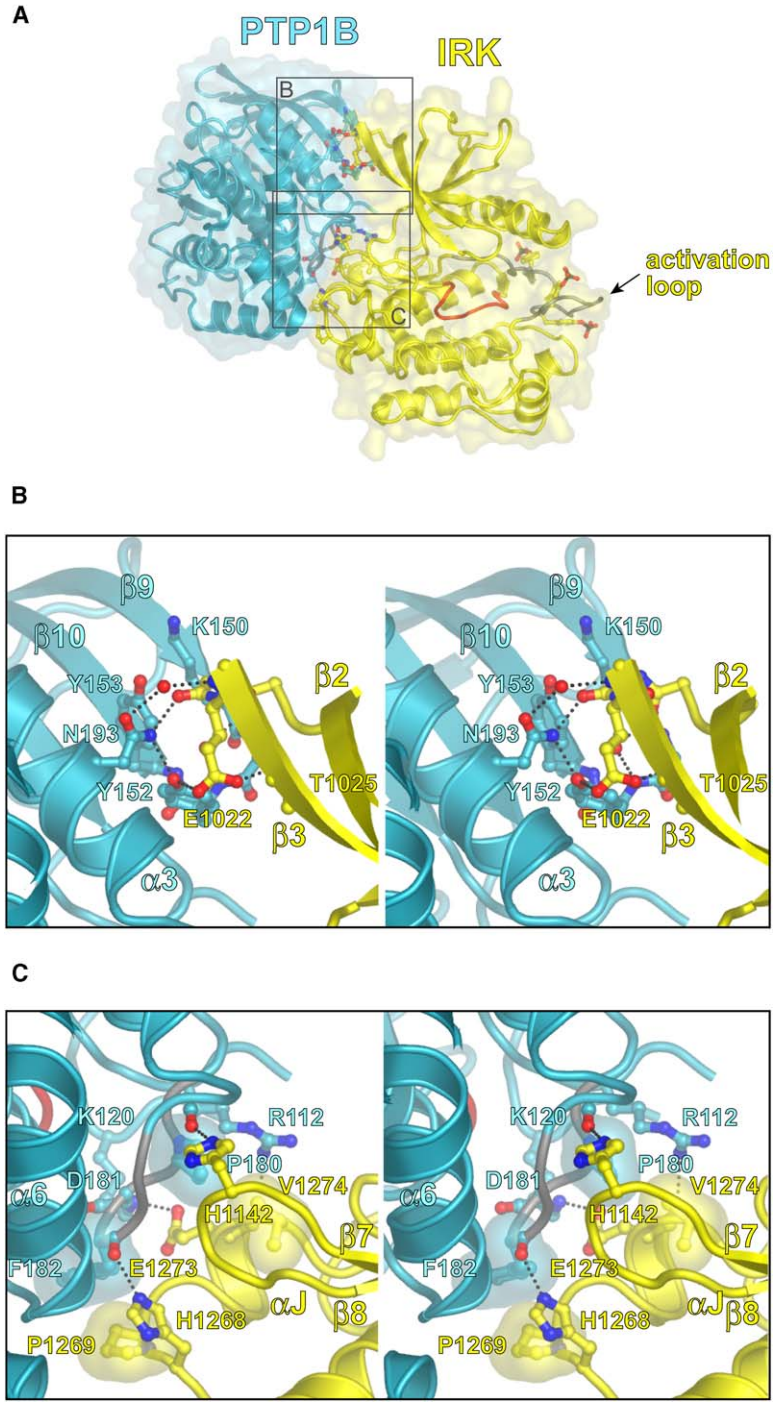

Figure 2. Interactions in the PTP1B-IRK Interface

(A) Overall view of the PTP1B-IRK interface with PTP1B and IRK shown in ribbon representation with semitransparent molecular surfaces. PTP1B is colored cyan, and IRK is colored yellow. The orientation is approximately half way between the upper and lower panels of Figure 1. The black rectangles indicate the zoom areas in (B) and (C). The catalytic loops of PTP1B and IRK are colored red, and the WPD and activation loops are colored gray.

(B) Stereoview of the interactions between the β2-β3 loop of IRK and the β9-β10 turn and α3 of PTP1B. Carbon atoms are colored cyan (PTP1B) or yellow (IRK), oxygen atoms are colored red, and nitrogen atoms are colored blue. Hydrogen bonds are represented by dashed lines.

(C) Stereoview of the interactions between αJ of IRK and the WPD loop of PTP1B. The coloring is the same as in (B).

and 118–119 adopt a different conformation than previously observed. This difference is likely due to the interaction of IRK with PTP1B residues in this region, namely, $R112^P$ and $K120^P$ (Figure 2C).

In most previous PTP1B structures, $E115^P$ (β5) is salt bridged to PTP-conserved $R221^P$ (α4). In the PTP1B-IRK structure, $R221^P$ is salt bridged to a sulfate ion rather than to $E115^P$. The lack of an E115-R221 salt bridge was also observed in the structure of the SHP1 phosphatase domain with bound phosphopeptide (Yang et al., 2000). In this case, residues of the peptide that are C-terminal to phosphotyrosine interact with the β5/β6 region of PTP1B, altering its conformation. Of note, in the PTP1B-IRK structure, the β5/β6 region is not sterically precluded by IRK from adopting the conventional conformation with an intact R221-E115 salt bridge.

Three well-ordered sulfate ions are bound to each PTP1B molecule (Figure 3B). One sulfate ion is located in the PTP1B active site, in the position of a substrate phosphate group. Another sulfate ion is located in the noncatalytic aryl pocket previously identified as a second phosphotyrosine binding site (Puius et al., 1997; Salmeen et al., 2000). The third sulfate ion is bound to

Table 2. Interactions in the PTP1B-IRK Interface

PTP1B Residue	Interactions with IRK
R112 (β4-β5 loop)	H bonded to E1273 backbone
K120 (β6-β7 loop)	Salt bridged to E1273 side chain
K150 (β9)	van der Waals contact with G1021
Y152 (β9-β10 turn)	H bonded to E1022 side chain
Y153 (β10)	van der Waals contact with G1021 backbone
P180 (WPD loop)	van der Waals contact with V1274 side chain
D181 (WPD loop)	van der Waals contact with E1273 side chain
F182 (WPD loop)	van der Waals contact with P1269 side chain
V184 (β11-α3 loop)	van der Waals contact with D1143 side chain
N193 (α3)	H bonded to G1021 backbone and A1023 backbone (water mediated)
R268 (α6)	H bonded to H1142 backbone
IRK Residue	**Interactions with PTP1B**
G1021 (β2-β3 loop)	van der Waals contact with K150 and Y153 side chains
E1022 (β2-β3 loop)	H bonded to Y152 side chain
P1102 (kinase insert)	van der Waals contact with D11 and K12 backbone
H1142 (β7-β8 loop)	H bonded to P185 backbone
D1143 (β7-β8 loop)	van der Waals contact with V184 side chain
H1268 (αI-αJ loop)	H bonded to F182 backbone
P1269 (αI-αJ loop)	van der Waals contact with F182 side chain
E1273 (αJ)	Salt bridged to K120 and van der Waals contact with D181 side chain
V1274 (αJ)	van der Waals contact with P180 side chain

Residues whose side chains are involved in interface contacts are listed on the left side. Cut-off distances are 3.2 Å for hydrogen bonds (H bonds) and 3.8 Å for van der Waals contacts.

$R221^P$, as mentioned above, and is also coordinated by $N111^P$ and $K120^P$.

IRK-IRK Interface

The two PTP1B-IRK complexes in the asymmetric unit, related by a noncrystallographic 2-fold axis, interact through a kinase interface comprising N-terminal lobe regions αC, the β3-αC loop, and the β4-β5 loop (Figure 4). The total surface area buried in this interface is 1575 $Å^2$, with a shape complementarity value of 0.64. The main contact element is αC, in which four hydrophobic residues, L1038, I1042, L1045, and A1048, interdigitate in antiparallel fashion with the corresponding residues from the other kinase molecule (Figure 4B). Hydrophobicity at all four positions is conserved in the insulin receptor subfamily (e.g., the IGF1 receptor), but not in other RTK subfamilies.

In addition to these interactions, several hydrogen bonds fortify the interface. R1041 in αC is hydrogen bonded to the backbone of the β4-β5 loop of the IRK dimer partner, and a backbone-backbone hydrogen bond is made between the β4-β5 loop of one IRK molecule and the β3-αC loop of the other molecule (Figure 4B). The side chain of Q1070 in the β4-β5 loop makes a long hydrogen bond (3.4 Å) with R1041 of the other IRK protomer. In this IRK dimer configuration, the activation loop phosphotyrosines are clustered inside the dimer, and the kinase active sites face outward and are unobstructed (Figure 1).

Comparison of the IRK Structure with Previous Structures

The structure of tris-phosphorylated IRK in the PTP1B-IRK complex is similar to the ternary structure of tris-phosphorylated IRK in complex with an ATP analog and peptide substrate (Hubbard, 1997), differing in two significant aspects: lobe closure and oligomeric state. With respect to IRK in the ternary structure, the N-terminal lobe of IRK is rotated toward the C-terminal lobe by ~9° in the PTP1B-IRK complex, i.e., the IRK structure in the complex is slightly more closed. This is evidently due to the imposition of the β9-β10 turn of PTP1B on the β2-β3 loop of IRK (Figures 2A and 2B). Because backside binding of PTP1B to IRK involves simultaneous engagement of both kinase lobes, this binding mode will be sensitive to the relative disposition of the two lobes. This could explain the observation that, in solution, PTP1B does not bind appreciably to unphosphorylated IRK (data not shown), in which the lobes are stabilized in an open state (Hubbard et al., 1994).

Previous crystal structures of IRK—wild-type, mutant, unphosphorylated, and phosphorylated—have all been of a monomeric kinase domain. In the PTP1B-IRK structure, a dimeric configuration of IRK is observed. Whether the two kinase domains in the holoreceptor stably interact as a dimer, either before or after insulin-triggered autophosphorylation, is not known. Upon autophosphorylation, the kinase-proximal juxtamembrane region of the insulin receptor disengages from a cleft between αC and the β sheet in the N-terminal kinase lobe, which exposes αC residues I1042, L1045, and A1048 (Li et al., 2003). These residues, along with L1038, form the IRK dimer interface (Figure 4B), suggesting the possibility that the dimeric state of IRK as observed in the PTP1B-IRK crystal structure could reflect the arrangement of the two activated kinase domains in the intact receptor.

Discussion

Specificity in the PTP1B-IRK Interface

The crystal structure of the PTP1B-IRK complex presented here reveals a noncatalytic mode of interaction between PTP1B and phosphorylated IRK, which is highly specific for these two proteins. From sequence alignments and the known structures of kinase domains of RTKs, only the insulin receptor subfamily contains the short α helix J at the end of the kinase domain, which redirects the polypeptide chain toward the backside of the kinase. Several residues in and preceding this helix in IRK contact the WPD loop of PTP1B (Figure 2C). Furthermore, a sequence alignment of insulin receptor subfamily members reveals that the IRK residues in the PTP1B-IRK interface are unique to the insulin receptor. Even the highly related IGF1 receptor, with 81% sequence identity in the tyrosine kinase domain, would not be predicted to engage PTP1B on the backside of the kinase domain because of substitutions at PTP1B-IRK interface residues G1021 (to D; β2-β3 loop), H1142 (to E; β7-β8 loop) and H1268 (to E; αI-αJ loop).

A sequence alignment of PTPs (Andersen et al., 2001) also highlights the specific nature of the PTP1B-IRK interface. Y152 (β9-β10 turn) and N193 (α3), which are hydrogen bonded to the β2-β3 loop of IRK (Figure 2B), are highly variable in the PTP family. In SHP2, for example, aspartic acid residues are found at the equivalent positions of Y152 and N193, which would be disfavored for IRK binding. In the WPD loop of PTP1B, F182 is in van

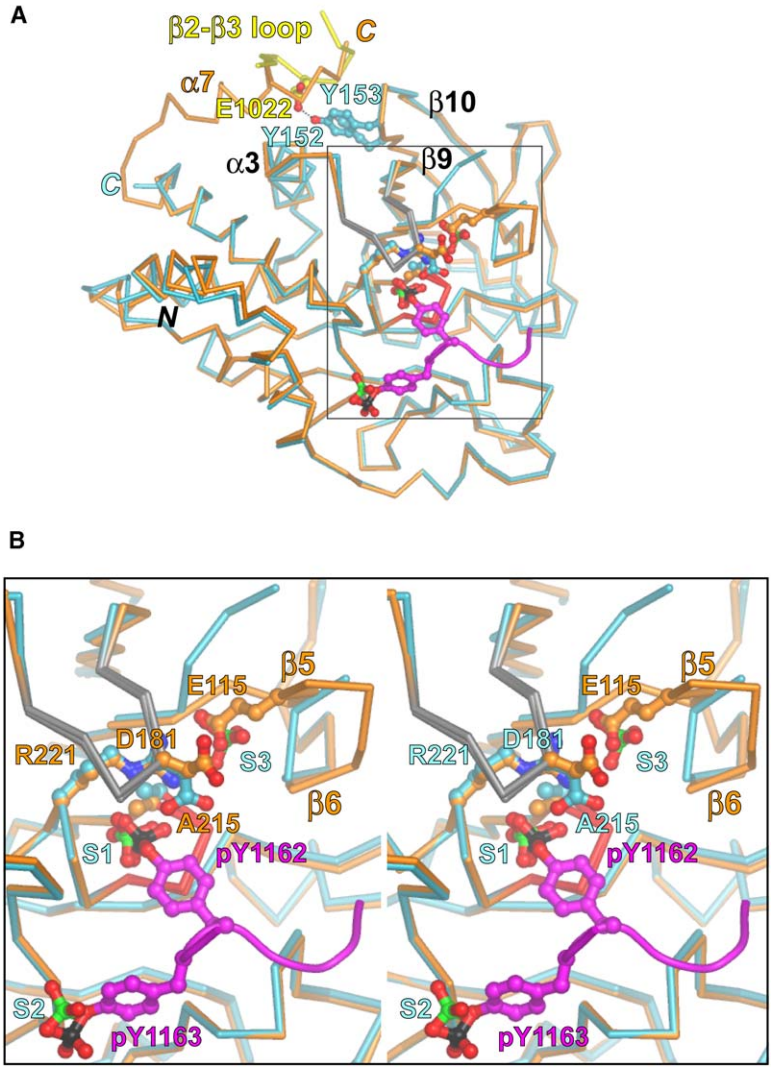

Figure 3. Superposition of PTP1B Structures

(A) The Cα trace of PTP1B from the PTP1B-IRK complex is colored cyan, and the superimposed Cα trace from the PTP1B-phosphopeptide structure (Salmeen et al., 2000) (PDB code 1G1F) is colored orange. The WPD loop (residues 179–184) in each PTP1B structure is colored gray, and the catalytic loop (residues 215–218) is colored red. The β2-β3 loop of IRK from the PTP1B-IRK structure is colored yellow, and the IRK phosphopeptide from the 1G1F structure is colored magenta. Select secondary structure elements are labeled, and the N and C termini of the two PTP1B structures are denoted by "*N*" and "*C*," respectively. The first ordered residue in both structures is E2, while the last ordered residue is M282 in the PTP1B-IRK structure and D298 in the 1G1F structure. Where termini or secondary structure elements overlap between the two PTP1B structures, the labels are colored black, otherwise they are colored cyan (PTP1B-IRK) or orange (1G1F). The black rectangle indicates the zoom area in (B).

(B) Stereoview near the active site of PTP1B. Select side chains of the two PTP1B structures, as well as the sulfate ions (labeled S1, S2, and S3) in the PTP1B-IRK structure, are shown in ball-and-stick representation. Carbon atoms are colored cyan (PTP1B from PTP1B-IRK), orange (PTP1B from 1G1F), or magenta (phosphopeptide from 1G1F), oxygen atoms are colored red, nitrogen atoms are colored blue, phosphorus atoms are colored black, and sulfur atoms are colored green.

der Waals contact with P1269 (αI-αJ loop) of IRK (Figure 2C). In PTPs, this residue is most often a histidine. TCPTP, which shares 70% sequence identity with PTP1B (residues 1–298), is the only other PTP that possesses the same key PTP1B-IRK interface residues (Y152, N193, P180, and F182). Recent biochemical studies with TCPTP-deficient cells have implicated TCPTP as well as PTP1B in the coordinated downregulation of insulin receptor signaling (Galic et al., 2005).

Possible Role for Backside Binding

The PTP1B-IRK crystal structure provides a plausible structural basis for the previously reported observations that Y152 and Y153 of PTP1B are determinants in the interaction of PTP1B with the insulin receptor (Bandyopadhyay et al., 1997; Dadke et al., 2000; Dadke and Chernoff, 2002). In the crystal structure, Y152 and Y153 interact with the β2-β3 loop of IRK (Figure 2B). Interestingly, insulin-stimulated phosphorylation of Y152 and Y153, for which there is biochemical evidence (Bandyopadhyay et al., 1997), would be predicted to abrogate backside binding of PTP1B to the insulin receptor.

In light of the biochemical data supporting a role for PTP1B residues Y152 and Y153 in the interaction with the insulin receptor, it is unlikely that the PTP1B-IRK interaction observed in the crystal structure is an artifact resulting from crystallization in ammonium sulfate (one of the most common protein crystallization agents). The significant buried surface area (1725 Å^2) and favorable shape complementarity (0.70), as well as two crystallographically independent copies of the PTP1B-IRK complex in the asymmetric unit, also argue for the physiologic relevance of the PTP1B-IRK interface. It appears that ammonium sulfate in the crystallization medium acted (serendipitously) to suppress the catalytic, phosphotyrosine-dependent interaction between PTP1B and IRK, revealing a noncatalytic mode of binding, which could be important for the selective recruitment of PTP1B to the insulin receptor.

PTP1B encounters the insulin receptor both as a single-chain receptor precursor in the ER and as a mature $\alpha_2\beta_2$ heterotetramer upon insulin-stimulated receptor endocytosis. It has been known for some time that the insulin receptor precursor is particularly sensitive to dephosphorylation by PTP1B, because of tethering of PTP1B to the ER (Lammers et al., 1993, 1997). Unlike most other RTKs, the insulin receptor precursor must undergo homodimerization in the ER in the course of

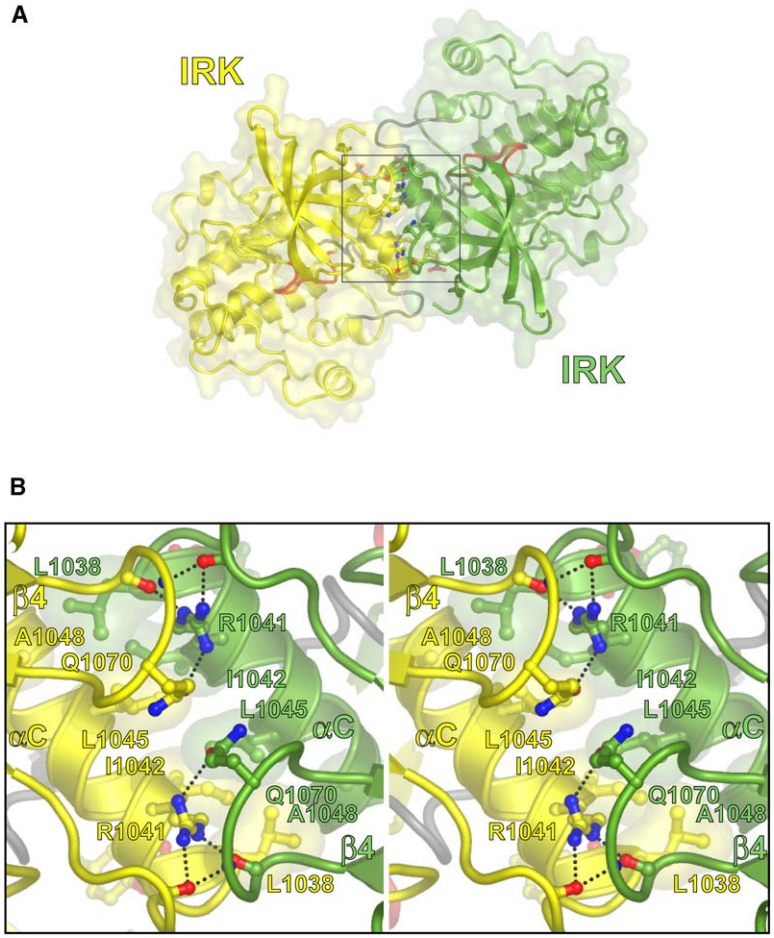

Figure 4. Interactions in the IRK-IRK Dimer Interface

(A) Overall view of the IRK dimer interface with each IRK protomer shown in ribbon representation with a semitransparent molecular surface. The two protomers are colored yellow and green. The orientation is the same as in the top panel of Figure 1. The black rectangle indicates the zoom area in (B).

(B) Stereoview of the interactions in the IRK dimer interface. Carbon atoms are colored yellow or green, oxygen atoms are colored red, and nitrogen atoms are colored blue. Hydrogen bonds are represented by dashed lines. The noncrystallographic 2-fold axis is perpendicular to the page, in the center of the diagram.

receptor maturation (intermolecular disulfide formation). Because of this requisite dimerization step, the potential exists for insulin-independent signaling by an activated (*trans*-phosphorylated) insulin receptor precursor.

Recent FRET (Romsicki et al., 2004) and BRET (Boute et al., 2003; Issad et al., 2005) experiments examining the interaction between PTP1B (trapping mutant) and the insulin receptor in living cells have demonstrated that there is a significant basal level of interaction between the two proteins, approximately half the insulin-stimulated level, which is due to PTP1B interacting with the insulin receptor precursor. Interestingly, addition of a catalytic site PTP1B inhibitor to cells substantially decreased the insulin-stimulated FRET signal between PTP1B and the insulin receptor, but not the basal FRET signal (Romsicki et al., 2004). This observation is suggestive of a noncatalytic mode of interaction between PTP1B and the insulin receptor precursor, such as that observed in the PTP1B-IRK crystal structure.

Although we were not able to detect binding of PTP1B to unphosphorylated IRK in solution, it is still possible that, in the context of an ER-tethered PTP1B and a transmembrane insulin receptor, appreciable backside binding of PTP1B to an unphosphorylated receptor might occur (reduced dimensionality effect), either to a mature heterotetramer in the plasma membrane or to a receptor precursor in the ER. This interaction mode could colocalize PTP1B to the insulin receptor for rapid dephosphorylation upon insulin-stimulated or adventitious receptor phosphorylation. Indeed, it is has been previously observed that the association between a PTP1B trapping mutant and the insulin-stimulated insulin receptor is rapid (~5 min) compared to the association of PTP1B with the PDGF (platelet-derived growth factor) and EGF (epidermal growth factor) receptors (~30 min) (Haj et al., 2002; Boute et al., 2003; Romsicki et al., 2004; Shi et al., 2004).

Another possible scenario is that PTP1B binds to the backside of a phosphorylated insulin receptor. Because of the high affinity of a PTP1B trapping mutant for phosphorylated IRK (front side binding: K_d ~100 nM, data not shown), any appreciable backside binding of wild-type PTP1B to a phosphorylated insulin receptor would require that the phosphotyrosine residues are protected from facile PTP1B dephosphorylation. Partial protection from dephosphorylation by PTPs, mediated by receptor dimerization, has been demonstrated for the PDGF receptor (Shimizu et al., 2001). The PTP1B-IRK structure presented here, in which the activation loop phosphotyrosines are sequestered in the center of the kinase dimer (Figure 1, bottom), provides a possible structural mechanism for phosphatase protection. Alternatively, insulin-stimulated oxidation of the catalytic cysteine (C215) in PTP1B (Meng et al., 2004) would disrupt the catalytic, phosphotyrosine-dependent interaction with the insulin receptor, and thus favor backside binding.

Spatially and temporally targeted biochemical experiments in cells will be necessary to determine the precise cellular context for backside binding and the functional consequences thereof.

Experimental Procedures

Protein Expression and Purification

The catalytic domain of PTP1B (residues 1–298), containing the substrate trapping mutation C215A, was purified from *E. coli* according to a protocol modified slightly from that reported previously (Barford et al., 1994). *E. coli* strain BL21(DE3) was transformed with the pET19b-PTP1B vector. An overnight culture was diluted 1:10 in fresh LB and grown at 37ºC. When OD_{600} reached 0.6, isopropylthiogalactopyranoside (IPTG) was added to a final concentration of 0.6 mM, and induction took place for 3 hr at 37ºC. Cells were collected by centrifugation at 5000 × g for 15 min. The cell pellet was resuspended in lysis buffer (20 mM imidazole [pH 7.5], 10% glycerol, 1 mM EDTA, 0.5 mM EGTA, 0.5 mM PMSF, 0.5 mM benzamidine, and 3 mM DTT) and passed through a French Press at 16,000 psi. The lysate was clarified by centrifugation at 15,000 × g for 40 min and loaded onto a Source-Q column (Amersham Biosciences) equilibrated in 20 mM imidazole (pH 7.5), 10% glycerol, 1 mM EDTA, 0.5 mM EGTA, 0.5 mM PMSF, 0.5 mM benzamidine, and 3 mM DTT. PTP1B was eluted by using a linear gradient of NaCl. PTP1B fractions were pooled and dialyzed against 25 mM sodium phosphate (pH 6.0), 10% glycerol, 1 mM EDTA, 0.5 mM EGTA, 0.5 mM PMSF, 0.5 mM benzamidine, and 3 mM DTT. PTP1B was then loaded onto a Source-S column (Amersham Biosciences) equilibrated in the same buffer and eluted by using a linear gradient of NaCl. Fractions containing PTP1B were pooled and exchanged into 20 mM Tris-HCl (pH 7.5), 50 mM NaCl, and 5 mM DTT and were concentrated to ~20 mg/ml in a Centricon-30 microconcentrator (Amicon). Production of tris-phosphorylated IRK was as previously described (Hubbard, 1997).

Crystallization, Data Collection, and Structure Determination

Purified PTP1B(C215A) and tris-phosphorylated IRK were mixed at a 1:1 molar ratio, as monitored by native gel electrophoresis, at a final protein concentration of ~5 mg/ml. Crystals of PTP1B and IRK were obtained by the hanging drop vapor diffusion method at 4ºC. A total of 1 or 2 μl stock protein complex was mixed with an equal volume of reservoir buffer (100 mM Tris-HCl [pH 7.5], 1.9 M ammonium sulfate, and 2% polyethylene glycol [PEG] 400) and was suspended over 500 μl reservoir buffer. Crystals appeared within several days and grew to maximum size (150 × 150 × 20 μm) in approximately 2 weeks. The crystals belong to primitive orthorhombic space group $P2_12_12_1$ with unit cell dimensions of a = 87.47 Å, b = 88.16 Å, c = 178.04 Å. There are two PTP1B and two IRK molecules per asymmetric unit, giving a solvent content of 50%.

Crystals were cryoprotected in 1.9 M ammonium sulfate, 100 mM Tris-HCl (pH 7.5), 9% sucrose, 2% glucose, 8% glycerol, and 8% ethylene glycol and were flash frozen in liquid propane. Data were collected from a single frozen crystal at beamline X25 at the National Synchrotron Light Source, Brookhaven National laboratory. All data were processed with DENZO and SCALEPACK (Otwinowski and Minor, 1997). The structure of the complex was determined by molecular replacement with the program AMoRe (Navaza, 1994) with previously determined structures for tris-phosphorylated IRK (1IR3) and PTP1B (1G1H) used as search models. Simulated-annealing, rigid-body, positional, and B factor refinement were carried out by using CNS (Brünger et al., 1998). Model building was performed with O (Jones et al., 1991). The atomic model for IRK includes residues 987–1283 in both copies in the asymmetric unit, and the atomic model for PTP1B includes residues 2–292 for one molecule, except for residues 115–116, and residues 2–282 for the other molecule, except for residues 115–117.

Acknowledgments

Support is acknowledged from the National Institutes of Health (DK052916 to S.R.H., CA058836 to J.C.). We thank M. Baumeister, N. Covino, S. Dadke, G. Dorsainville, J. Hu, R. Kohanski, and A. Stiegler for experimental support and discussions; J. Till and M. Becker for data collection assistance; and M. Mohammadi for critical reading of the manuscript.

Received: June 27, 2005
Revised: July 28, 2005
Accepted: July 28, 2005
Published: November 8, 2005

References

Ahmed, Z., Smith, B.J., Kotani, K., Wilden, P., and Pillay, T.S. (1999). APS, an adapter protein with a PH and SH2 domain, is a substrate for the insulin receptor kinase. Biochem. J. *341*, 665–668.

Andersen, J.N., Mortensen, O.H., Peters, G.H., Drake, P.G., Iversen, L.F., Olsen, O.H., Jansen, P.G., Andersen, H.S., Tonks, N.K., and Moller, N.P. (2001). Structural and evolutionary relationships among protein tyrosine phosphatase domains. Mol. Cell. Biol. *21*, 7117–7136.

Asante-Appiah, E., and Kennedy, B.P. (2003). Protein tyrosine phosphatases: the quest for negative regulators of insulin action. Am. J. Physiol. Endocrinol. Metab. *284*, E663–E670.

Bandyopadhyay, D., Kusari, A., Kenner, K.A., Liu, F., Chernoff, J., Gustafson, T.A., and Kusari, J. (1997). Protein-tyrosine phosphatase 1B complexes with the insulin receptor in vivo and is tyrosine-phosphorylated in the presence of insulin. J. Biol. Chem. *272*, 1639–1645.

Barford, D., Flint, A.J., and Tonks, N.K. (1994). Crystal structure of human protein tyrosine phosphatase 1B. Science *263*, 1397–1404.

Boute, N., Boubekeur, S., Lacasa, D., and Issad, T. (2003). Dynamics of the interaction between the insulin receptor and protein tyrosine-phosphatase 1B in living cells. EMBO Rep. *4*, 313–319.

Brünger, A.T., Adams, P.D., Clore, G.M., DeLano, W.L., Gros, P., Grosse-Kunstleve, R.W., Jiang, J.S., Kuszewski, J., Nilges, M., Pannu, N.S., et al. (1998). Crystallography & NMR system: a new software suite for macromolecular structure determination. Acta Crystallogr. D Biol. Crystallogr. *54*, 905–921.

Dadke, S., and Chernoff, J. (2002). Interaction of protein tyrosine phosphatase (PTP) 1B with its substrates is influenced by two distinct binding domains. Biochem. J. *364*, 377–383.

Dadke, S., Kusari, J., and Chernoff, J. (2000). Down-regulation of insulin signaling by protein-tyrosine phosphatase 1B is mediated by an N-terminal binding region. J. Biol. Chem. *275*, 23642–23647.

Ebina, Y., Ellis, L., Jarnagin, K., Edery, M., Graf, L., Clauser, E., Ou, J.H., Masiarz, F., Kan, Y.W., Goldfine, I.D., et al. (1985). The human insulin receptor cDNA: the structural basis for hormone-activated transmembrane signalling. Cell *40*, 747–758.

Elchebly, M., Payette, P., Michaliszyn, E., Cromlish, W., Collins, S., Loy, A.L., Normandin, D., Cheng, A., Himms-Hagen, J., Chan, C.C., et al. (1999). Increased insulin sensitivity and obesity resistance in mice lacking the protein tyrosine phosphatase-1B gene. Science *283*, 1544–1548.

Galic, S., Hauser, C., Kahn, B.B., Haj, F.G., Neel, B.G., Tonks, N.K., and Tiganis, T. (2005). Coordinated regulation of insulin signaling by the protein tyrosine phosphatases PTP1B and TCPTP. Mol. Cell. Biol. *25*, 819–829.

Gustafson, T.A., He, W., Craparo, A., Schaub, C.D., and O'Neill, T.J. (1995). Phosphotyrosine-dependent interaction of SHC and insulin receptor substrate 1 with the NPEY motif of the insulin receptor via a novel non-SH2 domain. Mol. Cell. Biol. *15*, 2500–2508.

Haj, F.G., Verveer, P.J., Squire, A., Neel, B.G., and Bastiaens, P.I. (2002). Imaging sites of receptor dephosphorylation by PTP1B on the surface of the endoplasmic reticulum. Science *295*, 1708–1711.

Hubbard, S.R. (1997). Crystal structure of the activated insulin receptor tyrosine kinase in complex with peptide substrate and ATP analog. EMBO J. *16*, 5572–5581.

Hubbard, S.R., Wei, L., Ellis, L., and Hendrickson, W.A. (1994). Crystal structure of the tyrosine kinase domain of the human insulin receptor. Nature *372*, 746–754.

Issad, T., Boute, N., Boubekeur, S., and Lacasa, D. (2005). Interaction of PTPB with the insulin receptor precursor during its biosynthesis in the endoplasmic reticulum. Biochimie *87*, 111–116.

Janin, J., and Chothia, C. (1990). The structure of protein-protein recognition sites. J. Biol. Chem. *265*, 16027–16030.

Jones, T.A., Zou, J.Y., Cowan, S.W., and Kjeldgaard, M. (1991). Improved methods for building protein models in electron density maps and the location of errors in these models. Acta Crystallogr. A *47*, 110–119.

Klaman, L.D., Boss, O., Peroni, O.D., Kim, J.K., Martino, J.L., Zabolotny, J.M., Moghal, N., Lubkin, M., Kim, Y.B., Sharpe, A.H., et al. (2000). Increased energy expenditure, decreased adiposity, and tissue-specific insulin sensitivity in protein-tyrosine phosphatase 1B-deficient mice. Mol. Cell. Biol. *20*, 5479–5489.

Kotani, K., Wilden, P., and Pillay, T.S. (1998). SH2-Bα is an insulin-receptor adapter protein and substrate that interacts with the activation loop of the insulin-receptor kinase. Biochem. J. *335*, 103–109.

Lammers, R., Bossenmaier, B., Cool, D.E., Tonks, N.K., Schlessinger, J., Fischer, E.H., and Ullrich, A. (1993). Differential activities of protein tyrosine phosphatases in intact cells. J. Biol. Chem. *268*, 22456–22462.

Lammers, R., Moller, N.P., and Ullrich, A. (1997). The transmembrane protein tyrosine phosphatase alpha dephosphorylates the insulin receptor in intact cells. FEBS Lett. *404*, 37–40.

Lawrence, M.C., and Colman, P.M. (1993). Shape complementarity at protein/protein interfaces. J. Mol. Biol. *234*, 946–950.

Li, S., Covino, N.D., Stein, E.G., Till, J.H., and Hubbard, S.R. (2003). Structural and biochemical evidence for an autoinhibitory role for tyrosine 984 in the juxtamembrane region of the insulin receptor. J. Biol. Chem. *278*, 26007–26014.

Liu, F., Hill, D.E., and Chernoff, J. (1996). Direct binding of the proline-rich region of protein tyrosine phosphatase 1B to the Src homology 3 domain of p130(Cas). J. Biol. Chem. *271*, 31290–31295.

Meng, T.C., Buckley, D.A., Galic, S., Tiganis, T., and Tonks, N.K. (2004). Regulation of insulin signaling through reversible oxidation of the protein-tyrosine phosphatases TC45 and PTP1B. J. Biol. Chem. *279*, 37716–37725.

Moodie, S.A., Alleman-Sposeto, J., and Gustafson, T.A. (1999). Identification of the APS protein as a novel insulin receptor substrate. J. Biol. Chem. *274*, 11186–11193.

Myers, M.P., Andersen, J.N., Cheng, A., Tremblay, M.L., Horvath, C.M., Parisien, J.P., Salmeen, A., Barford, D., and Tonks, N.K. (2001). TYK2 and JAK2 are substrates of protein-tyrosine phosphatase 1B. J. Biol. Chem. *276*, 47771–47774.

Navaza, J. (1994). AMoRe: an automated package for molecular replacement. Acta Crystallogr. A *50*, 157–163.

Otwinowski, Z., and Minor, W. (1997). Processing of x-ray diffraction data collected in oscillation mode. Methods Enzymol. *276*, 307–326.

Puius, Y.A., Zhao, Y., Sullivan, M., Lawrence, D.S., Almo, S.C., and Zhang, Z.Y. (1997). Identification of a second aryl phosphate-binding site in protein-tyrosine phosphatase 1B: a paradigm for inhibitor design. Proc. Natl. Acad. Sci. USA *94*, 13420–13425.

Romsicki, Y., Reece, M., Gauthier, J.Y., Asante-Appiah, E., and Kennedy, B.P. (2004). Protein tyrosine phosphatase-1B dephosphorylation of the insulin receptor occurs in a perinuclear endosome compartment in human embryonic kidney 293 cells. J. Biol. Chem. *279*, 12868–12875.

Salmeen, A., Andersen, J.N., Myers, M.P., Tonks, N.K., and Barford, D. (2000). Molecular basis for the dephosphorylation of the activation segment of the insulin receptor by protein tyrosine phosphatase 1B. Mol. Cell *6*, 1401–1412.

Saltiel, A.R., and Pessin, J.E. (2002). Insulin signaling pathways in time and space. Trends Cell Biol. *12*, 65–71.

Shi, K., Egawa, K., Maegawa, H., Nakamura, T., Ugi, S., Nishio, Y., and Kashiwagi, A. (2004). Protein-tyrosine phosphatase 1B associates with insulin receptor and negatively regulates insulin signaling without receptor internalization. J. Biochem. (Tokyo) *136*, 89–96.

Shimizu, A., Persson, C., Heldin, C.H., and Ostman, A. (2001). Ligand stimulation reduces platelet-derived growth factor beta-receptor susceptibility to tyrosine dephosphorylation. J. Biol. Chem. *276*, 27749–27752.

Tonks, N.K. (2003). PTP1B: from the sidelines to the front lines! FEBS Lett. *546*, 140–148.

Tonks, N.K., and Neel, B.G. (1996). From form to function: signaling by protein tyrosine phosphatases. Cell *87*, 365–368.

Ullrich, A., Bell, J.R., Chen, E.Y., Herrera, R., Petruzzelli, L.M., Dull, T.J., Gray, A., Coussens, L., Liao, Y.C., Tsubokawa, M., et al. (1985). Human insulin receptor and its relationship to the tyrosine kinase family of oncogenes. Nature *313*, 756–761.

White, M.F. (1998). The IRS-signalling system: a network of docking proteins that mediate insulin action. Mol. Cell. Biochem. *182*, 3–11.

Wiesmann, C., Barr, K.J., Kung, J., Zhu, J., Erlanson, D.A., Shen, W., Fahr, B.J., Zhong, M., Taylor, L., Randal, M., et al. (2004). Allosteric inhibition of protein tyrosine phosphatase 1B. Nat. Struct. Mol. Biol. *11*, 730–737.

Yang, J., Cheng, Z., Niu, T., Liang, X., Zhao, Z.J., and Zhou, G.W. (2000). Structural basis for substrate specificity of protein-tyrosine phosphatase SHP-1. J. Biol. Chem. *275*, 4066–4071.

Zabolotny, J.M., Bence-Hanulec, K.K., Stricker-Krongrad, A., Haj, F., Wang, Y., Minokoshi, Y., Kim, Y.B., Elmquist, J.K., Tartaglia, L.A., Kahn, B.B., and Neel, B.G. (2002). PTP1B regulates leptin signal transduction in vivo. Dev. Cell *2*, 489–495.

Accession Numbers

The coordinates and structure factors for the PTP1B-IRK crystal structure were deposited in the Protein Data Bank under code 2B4S.